Optimization Analysis of the Integrated Micro-coil Geometry Parameters Influence on the Uniformity of the Magnetic Field Distribution

Miha Gradišek and Janez Trontelj
Laboratory for Microelectronics, Faculty of Electrical Engineering, University of Ljubljana,
Tržaška cesta 25, 1000 Ljubljana, Slovenia
e-mails: Miha.Gradisek@fe.uni-lj.si, Janez.Trontelj1@guest.arnes.si

***Abstract*— The paper deals with the optimization of the integrated planar micro-coil characteristics with respect to maximizing the generated magnetic field amplitude and its uniformity along the region of interest. The integration calls for as efficient realization as possible otherwise the electrical heating would contribute to reduced performance of the integrated system in which the micro-coil is used. A multi-objective optimization is performed with respect to efficiency and uniformity of the magnetic field distribution. It is optimized in a range of the technological rules to be used in application where precise magnetic field measurement is required.**

Keywords-Integrated planar micro-coil; Magnetic field uniformity; Optimization; Parametrized 3D model.

I. INTRODUCTION

Whenever a new technological product is developed, the engineers strive for the best possible performance to price ratio. To accelerate product development and meet desired performance, various optimization methods are used. Based on the problem to be solved, two approaches are known, the stochastic and the deterministic approach. The former is used when the imitation and evolution of nature phenomenon is used during convergence to the optimal solution, while the latter minimizes or maximizes the criterion function, called the Objective Function (OF), with respect to the deterministic change of the independent Control Variables (CV) deterministically. This work uses a deterministic approach because the geometry of the integrated planar micro-coil (µCoil), realized in a standard Complementary Metal Oxide Semiconductor (CMOS) technology, is limited to the technological parameters dictated by the manufacturing process rules, so the inputs to the simulator are specific numbers and also the output of the simulator is determined by the Partial Differential Equation (PDE) formulation, therefore it is a deterministic object.

There has been a lot of research work on the uniformity of the magnetic field of coils in different constellations [1][2][3]. The most commonly used method to tackle magnetic field uniformity is accomplished with Helmholtz coils, which alleviate the difficulties in achieving the desired magnetic field homogeneity in the center of the system. On the other hand, coil integration in the CMOS process prevents a comparable relative precision of magnetic field variation, as it is inevitable to overcome the mismatch of the planar µCoil geometry as a result of the manufacturing process. Furthermore, the area of interest for magnetic field evaluation in Integrated Circuit (IC) is generally located outside the coil center plane, since the Hall sensor is located at the bottom of the IC, in the diffusion area, while the planar µCoil is realized at higher metal planes. Furthermore, the integration of the planar µCoil inside the die requires an energy efficient realization. Consequently, this work focuses not only on the optimization with respect to the uniformity of the magnetic field in the region of interest, but on electrical losses as a consequence of the µCoil resistance as well. These losses are reflected through the heat dissipation, which is particularly undesirable in the integrated system, where the µCoil is used as a generator of the reference magnetic field for the temperature calibration of the Application Specific Integrated Circuit (ASIC) for which the µCoil is to be used [4].

The paper is structured as follows: The Section II analyzes the optimization problem in relation to the specific ASIC and the possible formulation of the multi-objective function, the Section III describes the workflow from the design of 3D model of the µCoil to its integration into the optimization interface, while Section IV presents the simulation results with observations. Finally, the article concludes with summary of the overall work, and an acknowledgement.

II. OPTIMIZATION PROBLEM

As already mentioned, the integrated µCoil should exhibit high efficiency, i.e., it should generate as large magnetic flux density per µCoil bias current as possible. Therefore, we are staring to increase the magnetic flux density by increasing the number of coil turns N or to minimize the µCoil radius r. According to the Biot-Svart law, the axial component of the magnetic flux density B_Z in the centerline of the circumference is acquired after integration over all elements dL of the closed curve, e.g., µCoil (1) shown in Figure 1.

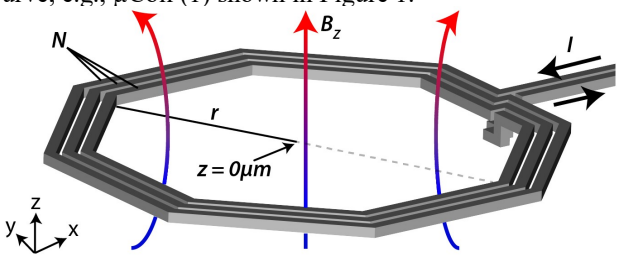

Figure 1. Parameters of the µCoil.

 ISBN: 978-1-61208-820-4

$$B_Z = \frac{\mu_0 INr}{4\pi\sqrt{(r^2+z^2)^3}} \oint dL. \quad (1)$$

Where, μ_0 is the permeability of free space, I current through N turns with radius r while z denotes the distance pointing from the center of the µCoil to an on-axis observation point. However, a higher number of µCoil turns N increases the total resistance R_{coil}, which means higher ohmic heat losses, or on the other hand larger variation of the magnetic flux density, B_Z when too small µCoil radius is chosen.

These variations are especially problematic when high uniformity of the magnetic field at the sensor location is desired, i.e., in the ASIC with temperature compensation of the Hall sensor and the overall system sensitivity. The Hall sensor is implemented in the strongly temperature dependent n-well diffusion region of the CMOS process. The sensitivity of the sensor to magnetic field is therefore temperature dependent, which is why a compensation technique should be introduced. The compensation approach is based on the simultaneous measurement of the external magnetic field and the reference magnetic field generated by the µCoil. Both signals are modulated at high frequency and later, after signal processing, demodulated back to a signal proportional to the external magnetic field and an additional signal containing information about Hall sensor sensitivity, based on the response of the overall ASIC sensitivity to a known reference magnetic field generated by the µCoil. The reference magnetic field should be constant over the entire modulation time. It should also be uniformly distributed over the entire Hall sensor volume, otherwise a parasitic signal component is sneaked into the signal of the measured magnetic field during the demodulation process. The aforementioned non-uniformity causes signal distortion, as shown in Figure 2, so the µCoil should generate as uniformly distributed reference magnetic field as possible. Taking into account the above criteria, an optimal realization of the µCoil should be designed, which calls for an optimization procedure.

The optimization should reduce µCoil resistance and at the same time decrease magnetic field gradient in the area of Hall sensor. Calculation of the rectangular cross-section planar µCoil resistance R_{COIL}, where current is not evenly distributed, as in wires with circular cross-section, is complicated therefore an electromagnetic simulator is mandatory. Objective function Q_R for the resistivity R_{coil} (2) has the minimum value of 0 for single turn coil N=1 with minimum radius r_{min}=10µm, which is half of the Hall sensor maximum dimension. Before the objective function Q_R is evaluated, the maximum, minimum R_{coil_min} and the average R_{coil_avg} resistance of the µCoil are determined in separate simulation run. The constant k_R is used to normalize the maximum value of Q_R compared to other objective function maximum.

$$Q_R = \frac{R_{COIL}-R_{MIN}}{R_{AVG}} * k_R \quad (2)$$

Objective function Q_{stdB}, which evaluates the uniformity of the magnetic field (3), is composed of the standard deviation of the magnetic flux density σ_B over the cross-section line where Hall sensor is positioned, marked in red in Figure 3. For comparable σ_B at different magnitudes of magnetic flux densities B_Z for different µCoil radius, the normalization of σ_B is accomplished by the magnetic flux density in the center of the µCoil B_{Z0}. The minimum $(\sigma_B/B_{Z0})_{MIN}$ and maximum $(\sigma_B/B_{Z0})_{MAX}$ ratios of standard deviation to magnetic flux density are again acquired in separate simulation runs to calculate $(\sigma_B/B_{Z0})_{AVG}$ as well. Normalization constant is represented by k_{stdB}.

$$Q_{stdB} = \frac{(\frac{\sigma_B}{B_{Z0}})-(\frac{\sigma_B}{B_{Z0}})_{MIN}}{(\frac{\sigma_B}{B_{Z0}})_{AVG}} * k_{stdB} \quad (3)$$

The purpose of the third objective function (4), which is composed of Q_R and Q_{stdB}, is to compare and find an optimal solution when both Q_R and Q_{stdB} have equal weight. Nevertheless, the objective function $Q_{combined}$ could be reformulated based on the design preferences for Q_R or Q_{stdB} to achieve a different significance of the specific objective function.

$$Q_{combined} = abs(1 - \frac{Q_R}{Q_{stdB}}) \quad (4)$$

All objective functions are formulated in such a way that they converge to 0 when the resistance (2) decreases, the relative uniformity of the magnetic flux density (3) decreases and when the two above mentioned function values converge to each other (4). Three objective functions form the multi-objective function $Q(r,N)$, for which the optimizer should find a minimum value (5). The optimizer search for the solution in the space of the possible parameters, i.e., the objective variables. Additionally, constraint of the minimum magnetic flux density B_{Z_min}=1mT in the region of Hall sensor from $-r_{min}$ to $+r_{min}$ is specified to attain sufficient magnetic field. The control variables ranges are listed in Table 1. All simulations are carried out for a µCoil bias current of 10mA.

$$min\, Q(r, N) \quad (5)$$

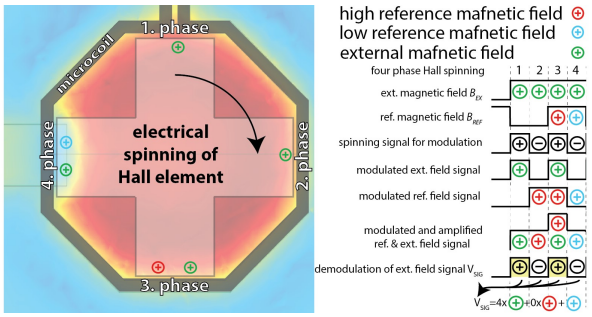

Figure 2. Influence of non-uniformly distributed reference magnetic field on the signal error.

TABLE I. OPTIMIZATION PARAMETERS

Control variable / Constraints	*Symbol*	*Lower bound*	*Upper bound*
µCoil radius	r	10 (µm)	50 (µm)
Number of µCoil turns	N	1	3

 ISBN: 978-1-61208-820-4

III. SIMULATION ENVIRONMENT

For the simulation purpose, Comsol Multiphysics in combination with Solidworks is used. The chart flow of the optimization procedure is presented in Figure 4.

Firstly, a parametrized 3D model of the µCoil is constructed in Solidworks according to the recommendation of the 0.35µm CMOS technology semiconductor foundry. The two most important parameters linked to the Comsol Multiphysics simulator are the µCoil diameter *r* and the number of µCoil turns *N*. The designed 3D model is imported into Comsol Multiphysics geometry, where the two parameters mentioned above are linked to the control variables that are permutated in the predefined range from the lower to the upper bound during optimization. The planar aluminum µCoil is inserted inside sphere where the electromagnetic evaluation takes place. The µCoil that is inserted into the sphere within the simulation environment with generated mesh is shown in Figure 3. The free tetrahedral mesh should be finer at the boundaries of the different domains and short edges, while it should be coarser, at other locations to avoid memory errors. Since the optimization problem is time independent, the evaluation of the electrical characteristics of the 3D µCoil model is performed by the Comsol Multiphysics "AC/DC Electromagnetic Fields" module with static analysis on the basis of Finite Element Method (FEM). This module is suitable for the calculation of the µCoil resistance and the generated magnetic field distribution, which are the main concerns and have to be considered during the optimization process. Simulator provides many optimization algorithms, but many of them tend to get stuck in local minima, as they iteratively converge to the local optimum [5], based on the value of the multi-objective function from the previous step, as shown in Figure 5. To overcome this problem, the optimization is performed using a Monte Carlo method that randomly sweeps the entire parameter search space with uniform distribution of solver points independently of the previous step to find global optimum. In the optimization interface, multi-objective functions (2-5) and an additional constraint of B_{Z_min} are specified.

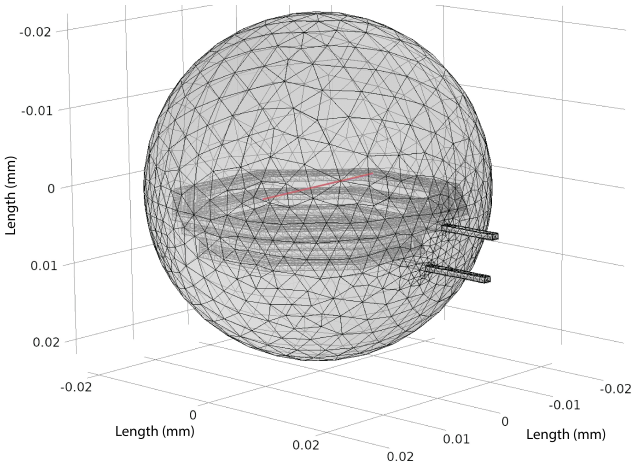

Figure 3. Quality of the mesh dictates accuracy of acquired model evaluation.

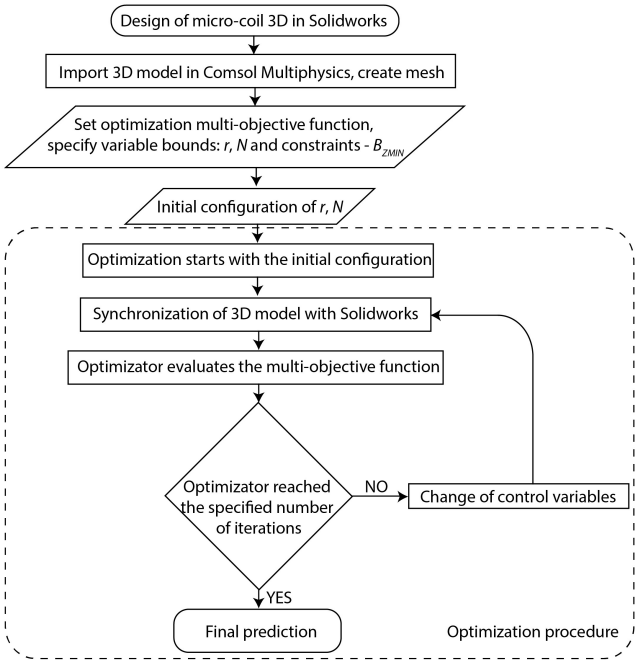

Figure 4. Flow chart of the µCoil parameters optimization.

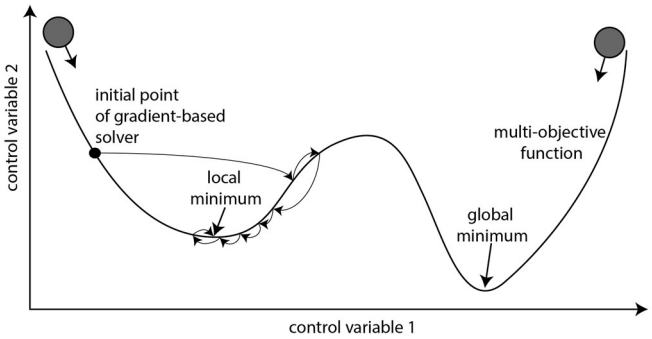

Figure 5. Local and global optimum.

During the optimization process the geometry of the µCoil is changed based on values of the control variable *r* and *N*. These two variables are permutated, while the statistical distribution of the values of the multi-objective function is acquired. The optimizer repeats the simulations as long as it does not reach the specified number of iterations.

IV. RESULTS

The optimization of the relatively simple geometry of the µCoil in combination with the Monte Carlo algorithm is quit time-consuming. In addition, the computing power increases exponentially with additional control variables. The optimizer therefore only works with the control variables that are essential for the optimization, while some parameters are evaluated and determined prior to the optimization run, e.g., shape of the µCoil structure, some CMOS technology data such as thickness of the specific metal layer, metal material, etc. The design rules specified in Process Design Kit (PDK),

 ISBN: 978-1-61208-820-4

within which the µCoil is developed, restrict the design of curves in the layout, consequently the planar µCoil consists of straight sides only. It can be seen from Figure 6 that variation in the number of sides of the µCoil has a negligible effect on B_z in the center of the µCoil, while the resistance listed in Table 2 decreases as the shape approaches the circumference shape. Table 2 summarizes resistivity for µCoil with N=1 and r=10µm. With regard to resistance and adoption to the maximum dimension of the Hall element, the octagon shape is chosen for the optimization process.

To further reduce the difficulty of the optimization process, four optimization runs were performed separately for each of the four IC metal layers. From the Table 3 where optimization results are given, it is evident when µCoil turn is closest to the Hall sensor, i.e., metal *m1,* the radius *r1* is larger than *r2* for the higher metal layer *m2*. This result is expected because the variations in magnetic flux density at the edge of the coil conductor are at least in the order of 10 greater than the variations in the center of the coil. As a result, the standard deviation of magnetic flux density in a configuration with a small radius and small distance between the source and the sensor of the magnetic field is larger compared to the configuration using the same distance with a larger radius or the same radius but larger distance, which is also shown in Figure 7. Figure 7 confirms that at greater distances between the source of the magnetic field and sensor course of the B_Z has flatter behavior compared to the same radius at smaller distances. Table 3 lists the number of turns on each metal layer, the values of all 3 objective functions and the average magnetic flux density B_Z on the line from $-r_{min}$ to $+r_{min}$ regarding the center of the Hall sensor. Resistance R_{coil} related to Q_R increases with larger radius or coil turns. Optimization without B_{Z_min} constraint results in an optimal solution for the radius in the middle radius search space range in combination with N=2 which is explained by the fact that the weight of both Q_R and Q_{stdB} is normalized. In contrary, optimization with the specified B_{Z_min} constraint, which is necessary to fulfill requirement of the real-world application, leads to a different design realization. Constraint B_{Z_min} cannot be achieved with higher metal levels m3 and m4 while m1 and m2 reach the desired magnitudes as shown in Table 3.

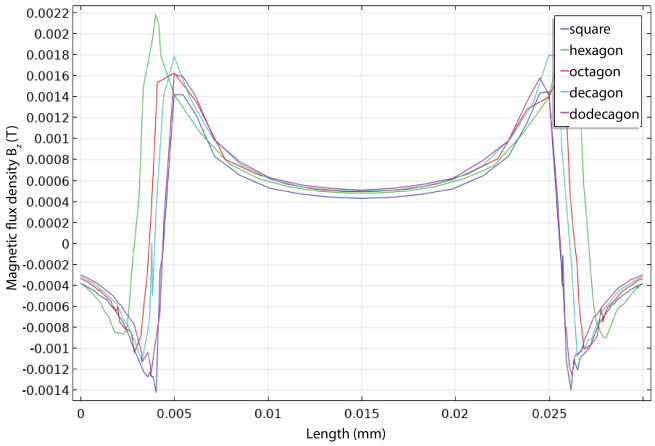

Figure 6. Magnetic flux density for different µCoil shape realizations (r=10µm, N=1).

TABLE II. COIL RESISTANCE FOR DIFFERENT NUMBER OF SIDES

Number of µCoil sides	*µCoil resistance (Ω)*
4	4.40
6	3.98
8	3.84
10	3.82
12	3.76

TABLE III. OPTIMIZATION SOLUTION

i	*Metal layer*	r_i *(µm)*	*N*	Q_R	Q_{stdB}	$Q_{combined}$	B_Z *(mT)*
1	m_i	14.3	3	0.253	0.413	1.053	1.017
2	m_i	12.2	3	0.209	0.363	0.998	1.055
3	m_i	10.6	2	0.084	0.049	0.860	0.643
4	m_i	10.0	3	0.159	0.330	1.007	0.646

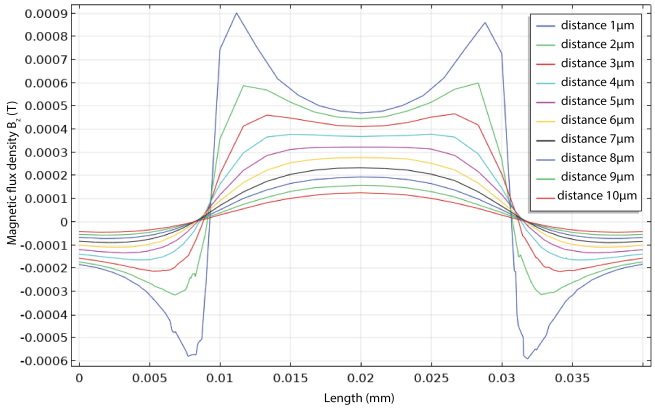

Figure 7. Magnetic flux density B_Z for different distances between magnetic field source and sensor (r=10µm, N=1).

Contribution to the magnetic flux densities of all four separately optimized µCoil layers is super positioned and verified with an additional simulation using the optimized 3D model shown in Figure 8. The total magnetic flux density of 3.76mT is close to the sum of all B_Z values listed in Table 3 which confirms our assumption.

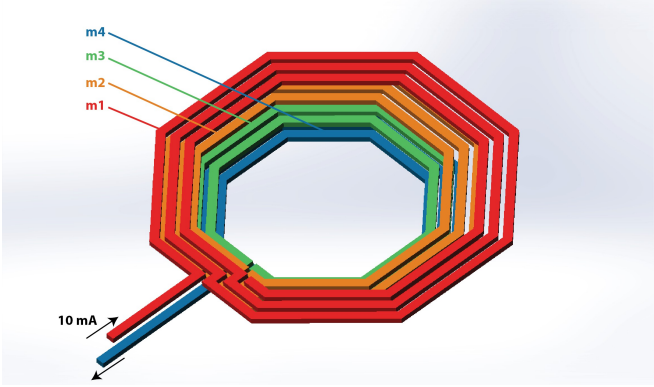

Figure 8. Acquired optimized 3D model of the planar µCoil realized at four metal layers.

 ISBN: 978-1-61208-820-4

The comparison between optimized and non-optimized µCoil is shown in Figure 9. The red line represents the non-optimized µCoil, while the blue line represents the optimized design. Both coils are designed to produce approximately the same average magnetic flux density B_Z=3.76mT. Streamline of magnetic flux density in the sphere volume of the simulation is shown in Figure 10, while magnetic flux density in the region of Hall sensor is shown in Figure 11.

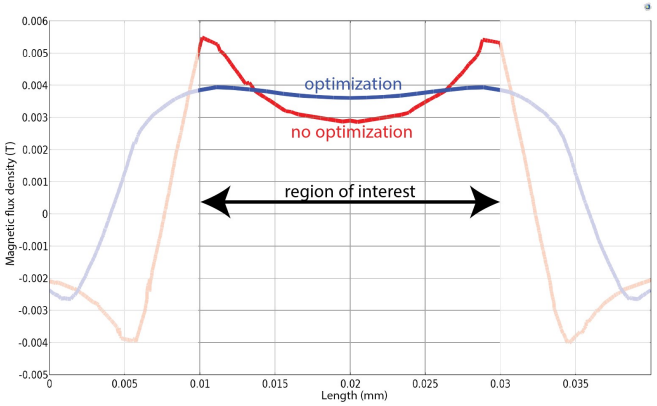

Figure 9. Comparison between optimized and non-optimized µCoil.

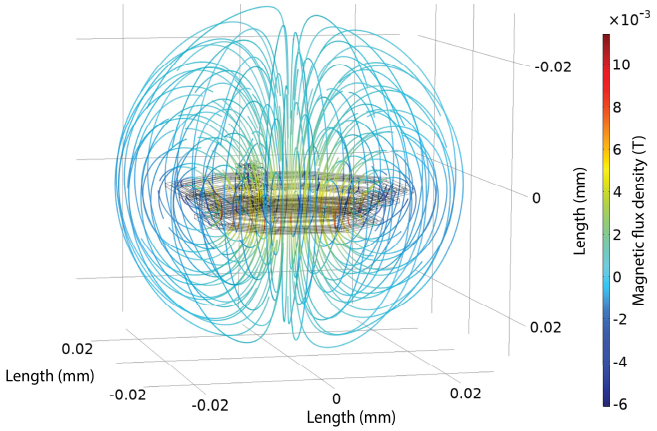

Figure 10. Streamline of magnetic flux density in the volume of simulation.

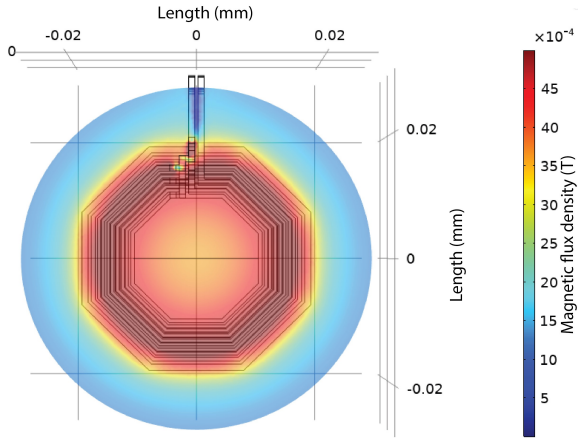

Figure 11. Distribution of magnetic flux density in plane of Hall sensor.

V. CONCLUSION AND FUTURE WORK

The behavior of the planar µCoil used in the ASIC, which incorporate temperature compensation of the sensor sensitivity, was analyzed. Presented work investigated the main disadvantage of on-chip generation of the magnetic field and proposed possible solutions obtained by an optimization process. The optimization was performed in Comsol Multiphysics using the 3D model designed in Solidworks. 3D model was optimized in terms of efficiency and performance to minimize thermal losses and maximize the magnetic field uniformity in the region of interest. The geometry of the 3D model was optimized in a range of possible parameters specified in the IC process. The multi-objective function and the constraints criterion could be modified based on the performance preferences of the µCoil in the specific application, which would lead to a different geometry of the optimized µCoil. Presented results indicated some deviations in magnetic flux density between separately optimized planar µCoils compared to the µCoil composed of all four planar µCoils. The deviations were due to the optimizer precision, as a coarser mesh was used in the composed version of µCoil otherwise too much memory was allocated for simulation run. The future work will focus on reformulating the 3D model meshing for a more efficient use of computer memory and a reasonable optimization time of more complex 3D structures.

ACKNOWLEDGMENT

The present work is part of the program “Systems on chip with integrated micromechanical, THz, magnetic and electrochemical sensors” No. P2-0257 (D) supported by Slovenian Research Agency (ARRS). Author would like to express gratitude to the LMFE department from the Faculty of Electrical Engineering in Ljubljana for expertise to greatly contribute to the success of the research.

REFERENCES

[1] B. J. Darrer, J. C. Watson, P. Bartlett, and F. Renzoni, “Toward an Automated Setup for Magnetic Induction Tomography,” IEEE Trans. Magn., vol. 51, no. 1, pp. 1–4, Jan. 2015, doi: 10.1109/TMAG.2014.2355420

[2] S. H. Kim and K. Ishiyama, “Magnetic robot and manipulation for active-locomotion with targeted drug release,” IEEE/ASME Transactions on Mechatronics,” vol. 19, no. 5, Oct. 2014, pp. 1651-1659, doi: 10.1109/TMECH.2013.2292595

[3] X. Han, Q. Cao, and L. Li, “Design and Evaluation of Three-Dimensional Electromagnetic Guide System for Magnetic Drug Delivery,” IEEE Trans. Appl. Supercond., vol. 22, no. 3, pp. 4401404, Jun. 2012, doi: 10.1109/TASC.2011.2176456

[4] M. Gradišek and J. Trontelj, “Integrated System Based on the Hall Sensors Incorporating Compensation of the Distortions,” Adv. Mater. Lett., vol. 11, no. 1, pp. 20011463 (1-4), Jan. 2020, doi: 10.5185/amlett.2020.011463

[5] A. Glotić, “Optimization of electrical power network elements by using evolutionary algorithms,” Ph.D dissertation, pp. 2-3, University of Maribor,” Maribor, 2011, [retrieved: Sep. 2020, https://dk.um.si/IzpisGradiva.php?lang=slv&id=18250]

 ISBN: 978-1-61208-820-4